A Stochastic Multi-Interval Scheduling Framework to Quantify Operational Flexibility in Low Carbon Power Systems

Sumanth Yamujala[1], Priyanka Kushwaha[3], Anjali Jain[1], Rohit Bhakar[1*], Jianzhong Wu[2], Jyotirmay Mathur[1]

[1] *Malaviya National Institute of Technology Jaipur, Rajasthan, India*
[2] *School of Engineering, Cardiff University, Cardiff, CF24 3AA UK*
[3] *ICF International Inc., New Delhi, India*

Abstract

Operational flexibility is required in power systems to mitigate load-generation imbalances. Inflexibility either results in infeasible scheduling or shift resources from their economic operating point. System operators must estimate flexibility requirement, assess its availability from committed resources, and take corrective measures to handle upcoming inflexibility events. Various metrics are integrated with economic dispatch to quantify different facets of flexibility- ramp, power, and energy. Consideration of all three facets is essential for its adequate assessment, but is often neglected in literature and requires an in-depth investigation. Further, existing literature hardly consider resources' day-ahead scheduling decisions while evaluating flexibility for real-time operations. This results in erratic assessment of available flexibility. In this context, the paper proposes a comprehensive metric to quantify flexibility in terms of ramp, power, and energy insufficiency by simultaneously considering their system-wide requirement and availability. A Resource Flexibility Index based on operating range and ramping capability of resources is proposed for accurate indication of available flexibility. The proposed metric is integrated with real-time stochastic multi-interval scheduling framework that considers day-ahead operational constraints. Netload forecast and associated uncertainty are characterized using Long Short-Term Memory and Markov Chain Monte Carlo techniques. Results highlight that the flexibility index is proportional to system's netload variability handling capability and average inflexibility can be reduced up to 97% with the utilization of emerging resources and ramp products. The proposed tools are of value to power system planners and operators to manage netload intermittency.

Keywords: Flexibility index, flexible resources, metrics, netload uncertainty, power system flexibility

Nomenclature

Sets and Indices

$B/b, n$ Set/index of bus, nodes b, n

*Corresponding Author. Tel: +91141-2713422. Address: Centre for Energy & Environment, Malaviya National Institute of Technology, JLN Marg, Jaipur - 302017, India

Email address: rbhakar.ee@mnit.ac.in (Rohit Bhakar[1])

D/d Set/index of ILDR

D'/d' Set/index of SLDR

E/e Set/index of BESS

H/h Set/index of PHES

I/i Set/index of conventional generation units

J/j Set/index of reduced netload scenarios

K/k Set/index of cost curve segments

M/m Set/index of 5-min time intervals for real-time dispatch

T/t Set/index of 15-min time intervals for day-ahead scheduling

χ Market participant, $\chi \in [D, D', E, H, I]$.

Constants and Parameters

C^{curt} Penalty for load curtailment ($)

C_i^{min} Minimum generation cost for unit i ($)

$C_i^{st/sd}$ Start-up/shut-down cost of unit i ($)

C_χ^{δ} Dispatch cost of residual capacity for χ ($), $\chi \in [D, D', E, H]$

N_m^f Forecasted netload at time m (MW)

$N_{m,j}$ Netload at time m and scenario j(MW)

$\overline{P}_\chi/\underline{P}_\chi$ Upper/lower power limits of χ (MW), $\chi \in [D, D', I]$

$\overline{P}_e^{(.)}/\underline{P}_e^{(.)}$ Upper/lower limit of BESS in charging and discharging modes ch/di (MW)

$r_i^{u/d/st/sd}$ Ramp limits of unit i (MW/5min)

$(.)_{i,m,j}$ DA scheduling binary status of unit i for running u/startup y/shutdown z

$Sl_{i,k}$ Slope of cost curve segment k for unit i

π_j Probability of reduced netload scenario j

$\overline{\varpi}_{b,n}$ Transmission line loading limit between bus b and node n (MVA)

$\lambda_m^{u/d}$ Maximum netload uncertainty in up/downward direction at time m (MW)

$\psi_{e,m,j}$ Charging status of BESS at time m and scenario j (0/1)

$\zeta_{e,m,j}$ Discharging status of BESS at time m and scenario j (0/1).

Variables

$\mathrm{E}^{s/\delta/\varphi}_{\chi,m,j}$	Energy availability through day-ahead schedule/re-schedule/commitment of χ at time m and scenario j (MWh)
$f^{u/d}_{\chi,m,j}$	Flexible ramp up/down allocation of resource χ at time m and scenario j (MW)
$L^{curt}_{b,m,j}$	Load curtailment at bus b in time m and scenario j (MWh)
$P^{s/\delta/\varphi}_{\chi,m,j}$	Scheduled/dispatched/committed power of χ at time m and scenario j (MW), $\chi \in [D, I]$
$P^{s+/\delta+}_{\chi,m,j}$ / $P^{s-/\delta-}_{\chi,m,j}$	Generation / consumption from Scheduled/re-dispatched power of χ at time m and scenario j (MW) , $\chi \in [D', E, H]$
$R^{A\_u/d}_{\chi,m,j}$	Available up/down ramping from χ at time m and scenario j (MW/5min)
$R^{C\_u/d}_{\chi,m,j}$	Capable up/down ramping from χ at time m and scenario j (MW/5min)
$R^{s/\delta/\varphi\_u/d}_{\chi,m,j}$	Scheduled/dispatched/ committed ramp in up/down direction of resource χ at time m and scenario j (MW/5 min)
$\alpha^{u/d}_{\chi,m,j}$	Up/down regulation schedule of unit χ at time m and scenario j (MW)
$\ell_{\chi,m,j}$	Reserve allocation of χ at time m and scenario j (MW)
$\tilde{(.)}_{m,j}$	Insufficiency of ramp R, power P and energy E at time m and scenario j (MW/5min, MW, MWh)
$\hat{(.)}_{m,j}$	Requirement for ramp R, power P and energy E (MW/5min, MW, MWh)
$(.)^{A}_{m,j}$	Power and energy availability at time m and scenario j (MW, MWh)
$\varpi_{b,n,m,j}$	Power flow at time m and scenario j in the line connecting bus b and node n (MVA)
$\lambda^{\delta/\varphi}_{\chi,m,j}$	Cost incurred for dispatching residual capacity (δ)/commitment (φ) of resource χ at time m and scenario j (\$)
$\phi_{b,m,j}$	Load angle of bus b at time m and scenario j (pu).

1. Introduction

Power systems are experiencing a strong growth in Renewable Energy Sources (RES) integration, especially solar and wind. Large-scale integration of such intermittent RES poses challenges to manage variability and uncertainty of netload *i.e.,* the difference between demand and RES generation. This underscores the need for *flexibility* to mitigate netload fluctuations and ensure reliable system operations. Flexibility is the energy, power, and ramp capability of a system to modify generation and/or demand in response to netload variations, at minimum cost [1]. Technically, the committed generation fleet should be able to handle netload variability, and provision of this additional flexibility should be economically viable. Although Conventional Generation (CG) units are providing flexibility in current scenario, transformation of energy systems towards the one dominated by RES requires flexibility to be harnessed from all aspects of power systems. System operations, Demand Response (DR), grid infrastructure upgradation, and integrating fast-start resources, Energy Storage Systems (ESS) and sector coupling can enhance flexibility [2, 3]. However, having sufficient flexible resources may not ensure their availability when required. Hence, power system operators need to estimate system flexibility requirement, assess its availability from committed resources, and take corrective measures to handle future system inflexibility events for reliable and secure system operations.

Indices like Loss of Load Expectation (LOLE) and Expected Energy not Served (EENS) reflect the reliability of a system based on firm capacity and outage rates of generators. These indices are applicable in planning horizon [4]. On the other hand, operational flexibility metrics highlight how an operational state of a resources' specific parameter contributes to power systems' ability in managing netload fluctuations or imbalances [5]. Various metrics have been proposed to quantify flexibility in both operational and planning time frames. Based on the focus of application, existing metrics evaluate operational flexibility by a) Flexibility requirement calculation b) Quantification of available flexibility and c) Flexibility insufficiency calculation.

The first category of metrics focus on evaluating flexibility requirement. Frequency spectrum based flexibility quantification methods are developed to assess multi-interval ramp and power requirements [6]. Energy storage requirement for flexibility in a planning horizon to balance netload fluctuations is assessed using Fourier transforms [7]. However, the methods are limited to planning studies. Flexibility requirement in terms of magnitude and duration of netload ramp *i.e.,* change in netload between two consecutive scheduling intervals are analyzed in [8–10]. Though resources are re-dispatched during Real-Time Economic Dispatch (RTED), in current practice the interval between market gate closure and re-dispatch is significantly large. This makes system's operating point uncertain at the dispatch interval prior to the scheduling time block. Also, netload variations correlate with RES generation. Existing methods do not consider these uncertain components between two consecutive scheduling intervals while quantifying ramp requirement. This may result in inaccurate ramp requirement estimation.

The second category of metrics attempt to quantify available flexibility using flexibility charts and ramping capability curves, based on installed capacity and operating point of generation mix. Such methods do not consider the effect of technical parameters on flexibility provision [11, 12]. Composite metric can rank CG units in a system by normalizing their technical parameters *viz.,* Minimum Stable Generation (MSG), Minimum Up/Down Times (MUT/MDT), Operating Range (OR), ramp-up/down and start-up/shut down time [13]. A similar flexibility index is formulated using fuzzy analytical hierarchy process [14]. However, ensuring flexibility results in certain additional operating cost and the composite metric is improved by considering both technical and

economic aspects [15]. The models normalize technical parameters (name plate parameters) of each generator based on the corresponding maximum and minimum values across the spectrum of available resources. Although these approaches rank generating units in terms of flexibility, they may not sufficiently provide *available flexibility level* as they cannot capture resources' scheduled power output. Also, among technical parameters, lower values of MSG, MUT/MDT and start up/shutdown times indicate higher system flexibility. On the other hand, OR and ramp up/down are positively correlated with system flexibility [15]. In short-term operational time frame, the latter can sufficiently highlight resource flexibility limits. System flexibility index only considers available flexibility in terms of ramping from emerging resources and CG units [16]. However, OR is neglected in the metric. Further, metrics in both the sets can either calculate flexibility requirement based on netload variations or flexibility available from conventional units. A comprehensive methodology that quantifies flexibility by simultaneously considering system-wide flexibility requirements and its availability from committed resources can provide better insights on upcoming inflexibility events and help system operators in making operational planning decisions.

The third category of metrics quantify system inflexibility using normalized flexibility index and loss of ramp probability [17–19]. Insufficient ramping resource expectation, similar to LOLE, is formulated to provide the probability that a power system cannot meet the changes in netload over a given time frame [20]. Magnitude of ramping insufficiency can be estimated using expected ramping insufficiency metric and dynamic uncertainty sets based flexibility assessment [21]. Ramp inflexibility can also be assessed by considering the economic implications of netload variability [22]. However, such methods are either limited to providing ramp insufficiency or do not estimate ramp requirement accurately, and need detailed simulations based on historic time series data. Also, metrics based on a single indicator cannot provide a comprehensive understanding of system-wide inflexibility [23]. Consideration of all three facets - ramp, power, and energy; is essential for appropriate assessment, but is often neglected in the literature [10]. Importance of considering energy limitations along with power and ramping capacities in systems with a significant share of energy-constrained resources is well highlighted [24]. Hence, an in-depth investigation on accurate flexibility assessment for all facets is required considering its system-wide requirement and availability from various flexible resources.

Most of the works integrate flexibility metrics in Real-Time (RT) dispatch models and optimize resources as an independent problem [17–19, 23]. Such dispatch models do not consider CG units' critical technical parameters like MUT/MDT or start-up/down times. This results in an erratic assessment of available flexibility. Moreover, consideration of residual/re-dispatchable capacity *i.e.,* difference between capable output and Day-Ahead (DA) schedule of resources, along with additional commitment of fast start units in RT can impact system flexibility assessment.

Further, in power systems with high share of RES, incorporating RT netload forecast is essential for both quantifying flexibility requirement and better re-dispatch decisions. Although utilizing improved forecasting techniques captures netload uncertainty, there exists a significant prediction error in DA forecasts [19]. Higher magnitude of uncertainty associated with increasing RES integration may affect the dispatch of committed units. Hence, a feedback from RT netload forecast must be incorporated in the RT scheduling framework, along with a consideration of DA operational constraints.

In this context, the paper quantifies flexibility in terms of all three facets considering RT netload forecasting and DA scheduling decisions of various flexible resources and CG units. The work contributes to develop:

- A comprehensive metric to quantify system inflexibility in terms of ramp, power and energy capability by simultaneous consideration of system-wide flexibility requirement and its availability from committed resources
- Resource Flexibility Index (RFI) based on operating range and ramping capability to highlight available flexibility of resources
- Stochastic multi-interval scheduling framework to dispatch resources considering RT netload forecasts and integrate the proposed flexibility assessment methodology.

Inflexibility is quantified as the difference between required and available values of ramp, power and energy. The corresponding required values of each facet are estimated from RT netload forecast and associated uncertainty characterization using Long Short-Term Memory (LSTM) and Markov Chain Monte Carlo (MCMC) techniques, respectively [25, 26]. Available flexibility is evaluated from the proposed stochastic multi-interval scheduling framework. The work helps system operators to analyze frequency and intensity of ramp, power, and energy inflexibility in upcoming scheduling intervals and provide a flexibility index between 0 and 1 to highlight available flexibility.

The rest of this paper is organized as follows- proposed flexibility assessment methodology and RFI are presented in Section II. Multi-interval scheduling framework is formulated in Section III. Section IV presents the case studies and Section V concludes the work.

2. Flexibility Quantification

Flexibility of a system depends on its system-wide requirement, technical characteristics of integrated resources as well as their operating state. Flexibility can be estimated as its insufficiency i.e., the difference between flexibility requirement and its availability. Hence, an accurate estimation of flexibility requirement and availability from resources is essential to assess its insufficiency. Major limitations of the existing literature are -

- Most of the existing flexibility metrics are developed on the consideration of limited parameters and provide ramping incapability of conventional units [16, 19, 20, 22]. With increasing integration of flexible resources, there is a need to consider additional two parameters of flexibility *i.e.,* power and energy. This helps to accurately quantify flexibility for the systems with significant share of energy-constrained sources *viz.,* energy storage and demand response.
- Although the inflexibility probability assessed by most of the metrics gives insight on flexibility, quantifying its magnitude on a wider parameter base would help system operators in taking corrective measures to ensure secure grid operations.
- Existing scheduling frameworks integrate flexibility metrics in economic dispatch and do not consider day-ahead scheduling decisions in the models [17–19, 23, 27]. Economic dispatch models do not consider critical technical parameters of conventional units such as minimum up/down time, start up/shut down time. Non-Consideration of these parameters may result in an over/false valuation of flexibility level. In practice, resource scheduling decisions are taken in day-ahead operations. Consideration of these scheduling decisions helps to assess actual system flexibility level in real-time.

- With increasing renewable integration, it is essential to harness flexibility from available and eligible resources to mitigate large variability from renewable energy sources. Limited literature has considered flexible resources for flexibility assessment [15, 16].

The proposed work addresses these limitations and quantifies flexibility insufficiency in terms of ramp, power and energy within a stochastic multi-interval Security Constrained Economic Dispatch (SCED) framework. Eqs. (1)-(4) quantify system-wide inflexibility in upward/downward ramping (MW/5 min), power (MW) and energy (MWh). Power and energy requirements are considered from real-time netload scenarios. Ramping requirement in up/downward directions is estimated from netload forecast and its associated uncertainty. Available flexibility is evaluated from resources' day-ahead scheduling decisions, residual capacity of online units, and additional commitment of fast start units.

$$\tilde{R}^{u}_{m,j} = \hat{R}^{u}_{m} - \sum_{\chi} R^{A\_u}_{\chi,m,j} \tag{1}$$

$$\tilde{R}^{d}_{m,j} = \hat{R}^{d}_{m} - \sum_{\chi} R^{A\_d}_{\chi,m,j} \tag{2}$$

$$\tilde{P}_{m,j} = \hat{P}_{m,j} - \sum_{\chi} P^{A}_{\chi,m,j} \tag{3}$$

$$\tilde{\mathrm{E}}_{m,j} = \hat{\mathrm{E}}_{m,j} - \sum_{\chi} \mathrm{E}^{A}_{\chi,m,j} \tag{4}$$

Further, eight technical parameters govern the resources available flexibility, especially generating units. They are ramp up and ramp down limits, OR, MSG, MUT, MDT, start up and shut down times. Consideration of all these technical parameters is important for ranking generating units based on their flexibility level [13–15, 17]. However, resource scheduling decisions are taken during day-ahead unit commitment, which considers start up and shut down times along with MUT and MDT of CG units. Additional unit commitment to meet load-generation imbalances in RT is carried out for only fast start units, hence the four parameters have limited impact on RT flexibility assessment. Varying MSG of units necessitates retrofitting, and usually it is assumed to be constant. In order to mitigate netload variations, committed resources must change their operating point based on the economic re-dispatch decisions. This capability depends on ramping up/down ability and operating range of resources. Hence, ramping and operating range are the three critical parameters that govern the available flexibility level of a resource. In this context, two resource flexibility indices (RFI) based on OR and ramping are developed to indicate available flexibility of committed resources. Further, lower index for OR also highlights the inflexibility due to MSG.

The adopted min-max normalization method covert indices to an identical range between 0 and 1, as given in (5)-(6). Unlike existing works, corresponding unit's maximum and minimum limits are taken in (5)-(6) for normalization. OR index (5) near 0 represents resource inflexibility in MSG ($\underline{P}_{\chi}$) or MUT/MDT, while the value near 1 highlights resource insufficiency in ramping up in case of sudden increase in demand. Similarly, a higher value of (6) indicates system's capability in utilizing available ramping. Generating units and flexible resources can ramp up or ramp down. However, for a given scheduling interval and netload, they can utilize any of the two capabilities. Hence to ensure proper normalization, average ramping capability of a resource is considered in

the denominator of (6).

$$RFI_{\chi}^{OR} = \sum_{j}^{J}\sum_{m}^{M} \pi_j \left[\frac{(P^{A}_{\chi,m,j} - \underline{P}_{\chi})}{(\overline{P}_{\chi} - \underline{P}_{\chi})} \right] \tag{5}$$

$$RFI_{\chi}^{ramp} = \sum_{j}^{J}\sum_{m}^{M} \pi_j \left[\frac{(R^{A\_u}_{\chi,m,j} + R^{A\_d}_{\chi,m,j})}{0.5(R^{C\_u}_{\chi,m,j} + R^{C\_d}_{\chi,m,j})} \right] \tag{6}$$

3. Multi-Interval stochastic SCED Framework

The proposed flexibility assessment methodology, (1-6), is integrated into a two-stage flexibility constrained scheduling framework with a 15-minute temporal DA - Security Constrained Unit commitment (DA-SCUC) and a 5-minute temporal Stochastic RT - Security Constrained Economic Dispatch (RT-SCED). Flexibility enhancement options like Battery Energy Storage Systems (BESS), Pumped Hydro Energy Storage (PHES), interruptible and shiftable load type DR are considered along with CG units. Fig. 1 outlines the proposed methodology. CG units and flexible resources along with wind and solar generation are scheduled in DA to meet 100% anticipated electricity demand and ancillary services. In DA-SCUC, energy, regulation, spinning reserve and Flexible Ramp Products (FRPs) are co-optimized. RT-SCED cannot be solved independently as resource dispatch decisions are bounded to DA schedules. Hence DA decisions are given as input to RT-SCED to highlight the impact of resources technical parameters on both dispatch and flexibility assessment. The 96 scheduling decisions of each resource for a complete day are converted into 288 dispatch decisions (5-minute resolution) considering resources scheduled and rated ramp limits. This data in 5-minute resolution is given as input to Stage-II *i.e.,* stochastic RT-SCED. This conversion do not violate the DA scheduling decisions. Resource scheduling inputs are same for each scenario. Along with resource schedule, RT netload profile forecasted from LSTM and associated uncertainty characterized using MCMC are utilized for Stage-II simulations. RT-SCED schedules additional CG units and residual capacity from resources along with DA schedule to fulfill stochastic netload. This scheduling framework provides resource dispatch decisions and information on system inflexibility. DA scheduling constraints are presented in Appendix-A. Operational constraints corresponding to RT-SCED are presented in this section-

3.1. Objective Function

The proposed RT- stochastic SCED minimizes the additional costs incurred due to dispatch of residual capacity, additional commitment of resources along with the penalties for load and RE curtailments and ramp up/down insufficiency, given in (7)

$$\lambda^{RT} = \sum_{j}^{J}\sum_{m}^{M} \left[\{\sum_{b}^{B} (L^{curt}_{b,m,j}) + \tilde{R}^{u}_{m,j} + \tilde{R}^{d}_{m,j}\} \pi_j C^{curt} + \pi_j \{\sum_{i}^{I} \lambda^{\varphi}_{i,m,j} + \sum_{\chi,\chi\notin i} \lambda^{\delta}_{\chi,m,j}\} \right] \tag{7}$$

$$\lambda^{\varphi}_{i,m,j} = (C^{st}_{i} y'_{i,m,j} + C^{sd}_{i} z'_{i,m,j}) + C^{\min}_{i} u'_{i,m,j} + \sum_{k}^{K} Sl_{i,k} (P^{\delta}_{i,k,m,j} + P^{\varphi}_{i,k,m,j}) \tag{8}$$

$$\lambda^{\delta}_{\chi,m,j} = C^{\delta}_{\chi}(P^{\delta}_{\chi,m,j}) \quad \forall\, \chi \notin i \tag{9}$$

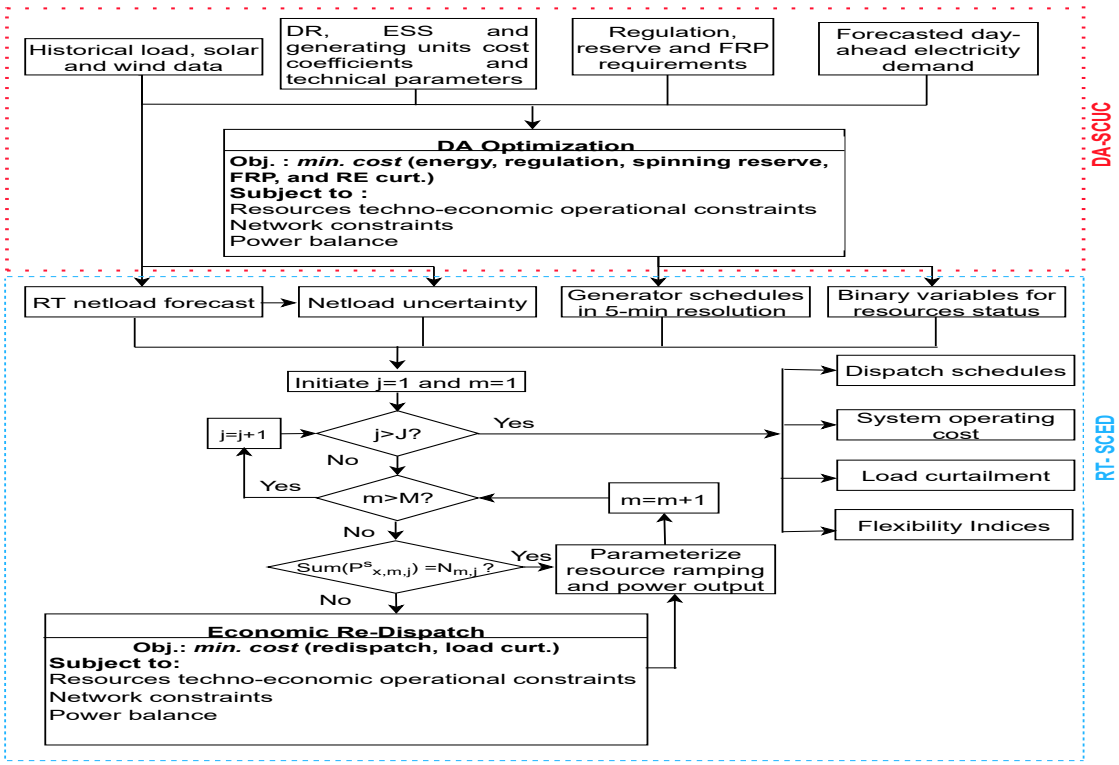

Figure 1: Proposed methodology for flexibility assessment

The first term of (7) gives the penalty for load curtailment, ramp up and down insufficiency. The second term gives the additional cost incurred in dispatching CG units and flexible resources, given in (8) and (9). Eq. (8) represents the linearized form of operating cost with the first term representing cost of additional start-up and shutdown of conventional units. Second part of (8) gives the cost incurred for committed conventional units to operate at MSG. Third term of (8) represents the linearized form of operating cost for committed CG units as well as for additional dispatch of committed units, where $\sum_{k}^{K} P^{\delta/\varphi}_{i,k,m,j} = P^{\delta/\varphi}_{i,m,j}$. The quadratic cost curve of CG units is divided into K segments having a slope of $Sl_{i,k}$ using piece-wise linearization. $u'_{i,m,j}$, $y'_{i,m,j}$ and $z'_{i,m,j}$ indicate operating, start-up and shut down status of additionally committed unit i in RT.

3.2. Ramp Requirement Calculations

3.2.1. Ramp Requirement

Unlike existing flexibility metrics, the proposed work estimates ramp requirement from the net-load variation between two consecutive scheduling intervals considering their extreme uncertainty. Eqs. (10)-(11) give the ramp requirement estimation [28]-

$$\hat{R}^{u}_{m} = max\left\{0, (N^{f}_{m} + \lambda^{u}_{m}) - (N^{f}_{m-1} - \lambda^{d}_{m-1})\right\} \tag{10}$$

$$\hat{R}^{d}_{m} = max\left\{0, (N^{f}_{m-1} + \lambda^{u}_{m-1}) - (N^{f}_{m} - \lambda^{d}_{m})\right\} \tag{11}$$

N^f_m and N^f_{m-1} is the forecasted netload at intervals m and $m-1$. λ^u_m and λ^d_{m-1} is the maximum upward/downward uncertainty at intervals m and $m-1$, respectively. Eq. (10) estimates the ramp up requirement. It is positive for netload movement in positive direction *i.e.,* $(N^f_m + \lambda^u_m) > (N^f_{m-1} - \lambda^d_{m-1})$, else it takes zero value. Similar condition is for ramp down requirement. This formulation considers total range of netload variability, and ramp requirement remains same for each scenario.

3.2.2. Ramp Capability

Ramping capability of committed resources for each netload scenario j is assessed using (12) and (13). Capable ramping is evaluated as the minimum of ramping capability and available operating range of resources. $u_{\chi,m,j}$, $y_{\chi,m,j}$ and $z_{\chi,m,j}$ indicate operating, start-up and shut down status of resource χ, obtained from DA-SCUC. During start up or shut down, corresponding ramping of units r^{st}_χ or r^{sd}_χ are considered.

$$R^{C\_u}_{\chi,m,j} = min\left\{(r^u_\chi u_{\chi,m-1,j} + r^{st}_\chi y_{\chi,m,j}), (\overline{P}_\chi - P^s_{\chi,m-1,j})u_{\chi,m,j}\right\} \tag{12}$$

$$R^{C\_d}_{\chi,m,j} = min\{(r^d_\chi u_{\chi,m,j} + r^{sd}_\chi z_{\chi,m,j}), (P^s_{\chi,m-1,j} - \underline{P}_\chi)(u_{\chi,m,j} + z_{\chi,m,j})\} \tag{13}$$

3.2.3. Ramp Availability

Available ramping is evaluated from the scheduled and residual ramp of resource χ for each scenario j along with the ramp available from additional commitment of resources, given in (14) and (15). Resources ramping in different scheduling options is calculated based on the change in corresponding power generation output between two consecutive dispatch intervals, given in (16) and (17)

$$R^{A\_u}_{\chi,m,j} = R^{s\_u}_{\chi,m,j} + R^{\delta\_u}_{\chi,m,j} + R^{\varphi\_u}_{\chi,m,j} \tag{14}$$

$$R^{A\_d}_{\chi,m,j} = R^{s\_d}_{\chi,m,j} + R^{\delta\_d}_{\chi,m,j} + R^{\varphi\_d}_{\chi,m,j} \tag{15}$$

$$R^{s/\delta/\varphi\_u}_{\chi,m,j} = P^{s/\delta/\varphi}_{\chi,m,j} - P^{s/\delta/\varphi}_{\chi,m-1,j} \tag{16}$$

$$R^{s/\delta/\varphi\_d}_{\chi,m,j} = P^{s/\delta/\varphi}_{\chi,m-1,j} - P^{s/\delta/\varphi}_{\chi,m,j} \tag{17}$$

Similarly, available power and energy capacity, $P^A_{\chi,m,j}$ and $\mathrm{E}^{\mathrm{A}}_{\chi,\mathrm{m,j}}$, are taken as the sum of scheduled , dispatched and committed power and energy capacities.

3.3. Resource Constraints

3.3.1. Generator Constraints

Eqs. (18) and (19) give the generator's maximum and minimum technical limits and feasible operating range for allocating energy, regulation, spinning reserve, and FRP. (20) and (21) ensure that change in power generation and allocation of regulation, reserve & FRP are within generator's ramp up r^u_i and ramp down r^d_i limits. At start up/shutdown time of unit, respective ramping r^{st}_i/r^{sd}_i are considered.

$$P^{s/\varphi}_{i,m,j} + P^{\delta}_{i,m,j} + \alpha^u_{i,m,j} + \ell_{i,m,j} + f^u_{i,m,j} \leq \overline{P}_i u_{i,m,j} \quad \forall i,m,j \tag{18}$$

$$P^{s/\varphi}_{i,m,j} - P^{\delta}_{i,m,j} - \alpha^{d}_{i,m,j} - \ell_{i,m,j} - f^{d}_{i,m,j} \geq \underline{P}_i u_{i,m,j} \quad \forall i,m,j \tag{19}$$

$$\begin{aligned} &P^{s/\varphi}_{i,m,j} - P^{s/\varphi}_{i,m-1,j} + P^{\delta}_{i,m,j} - P^{\delta}_{i,m-1,j} + \alpha^{u}_{i,m,j} + \ell_{i,m,j} + f^{u}_{i,m,j} + \\ &f^{d}_{i,m-1,j} \leq r^{u}_{i}(u_{i,m-1,j} + u'_{i,m-1,j}) + r^{st}_{i}(y_{i,m,j} + y'_{i,m,j})\, \forall i,m,j \end{aligned} \tag{20}$$

$$\begin{aligned} &P^{s/\varphi}_{i,m-1,j} - P^{s/\varphi}_{i,m,j} + (P^{\delta}_{i,m-1,j} - P^{\delta}_{i,m,j}) + \alpha^{d}_{i,m,j} + f^{d}_{i,m,j} + \\ &f^{u}_{i,m-1,j} \leq r^{d}_{i}(u_{i,m,j} + u'_{i,m,j}) + r^{sd}_{i}(z_{i,m,j} + z'_{i,m,j}) \quad \forall i,m,j \end{aligned} \tag{21}$$

3.3.2. BESS Constraints

BESS is modeled considering its State of Charge (SOC) in DA-SCUC as given in (A.13)-(A.18). Based on the DA schedules, redispatch is carried out by considering battery's maximum and minimum limits in charging and discharging modes, given in (22) - (23). Inclusion of $P^{\delta}_{e,m,j}$ changes the SOC of BESS and hence its dispatch is monitored through SOC, given in (24). Constraints (22)-(23) ensure that charging or discharging power, regulation, spinning reserve, and FRP does not exceed the rated power capacity of BESS. $\overline{P}^{ch}_{e}$, $\overline{P}^{di}_{e}$ and $\underline{P}^{ch}_{e}$, $\underline{P}^{di}_{e}$ are maximum and minimum power limits in charging/discharging modes, respectively. SOC of BESS at the end of scheduling day is assumed to reach its initial value. $P^{ch}_{e,m,j}$ and $P^{di}_{e,m,j}$ is the total scheduled power allocation of BESS for energy and ancillary services *i.e.*, $P^{ch}_{e,m,j} = P^{s-}_{e,m,j} + \alpha^{d}_{e,m,j} + f^{d}_{e,m,j}$ and $P^{di}_{e,m,j} = P^{s+}_{e,m,j} + \alpha^{u}_{e,m,j} + \ell_{e,j,m} + f^{u}_{e,m,j}$. Here Δm in eq. (24) is $\frac{1}{12}$.

$$P^{s-}_{e,m,j} + P^{\delta-}_{e,m,j} + \alpha^{d}_{e,m,j} + f^{d}_{e,m,j} \leq \overline{P}^{ch}_{e}\psi_{e,m,j} \quad , \quad P^{s-}_{e,m,j} \geq \underline{P}^{ch}_{e}\psi_{e,m,j} \quad \forall e,m,j \tag{22}$$

$$P^{s+}_{e,m,j} + P^{\delta+}_{e,m,j} + \alpha^{u}_{e,m,j} + \ell_{e,m,j} + f^{u}_{e,m,j} \leq \overline{P}^{di}_{e}\zeta_{e,m,j} \quad , \quad P^{s+}_{e,m,j} \geq \underline{P}^{di}_{e}\zeta_{e,m,j} \quad \forall e,m,j \tag{23}$$

$$SOC_{e,m,j} = SOC_{e,m-1,j} + \left\{(P^{ch}_{e,m,j} + P^{\delta-}_{e,m,j})\eta^{ch}_{e} - (P^{di}_{e,m,j} + P^{\delta+}_{e,m,j})/\eta^{di}_{e}\right\}\Delta m, \quad \forall m \tag{24}$$

3.3.3. PHES Constraints

Power generated and consumed from PHES is calculated using heads of the upper and lower reservoirs and the quantity of water discharge in generating and motoring modes. Change in the head of upper and lower reservoirs are modeled as SOC. Detailed modeling of PHES for DA-SCUC is presented in (A.19)-(A.24) [29]. Maximum power generation/consumption in generating/motoring modes is given in (25) and (26). Similar to BESS modeling, PHES dispatch is limited by the water head of both upper and lower reservoirs. $P^{prod}_{h,m}$ and $P^{cons}_{h,m}$ are the generation and motoring capability of PHES h at time m obtained from DA scheduling.

$$P^{s+}_{h,m,j} + P^{\delta+}_{h,m,j} + \alpha^{u}_{h,m,j} + \ell_{h,m,j} + f^{u}_{h,m,j} \leq P^{prod}_{h,m} \tag{25}$$

$$P^{s-}_{h,m,j} + P^{\delta-}_{h,m,j} + \alpha^{d}_{h,m,j} + f^{d}_{h,m,j} \leq P^{cons}_{h,m} \tag{26}$$

3.3.4. Demand Response Constraints

Interruptible Load DR (ILDR) and Shiftable Load DR (SLDR) models are implemented for the studies. (27)-(29) give the operating constraints of interruptible load type DR. (27) and (28) ensure that energy, regulation, spinning reserve, and FRP procurement from aggregated ILDR at each bus b are within maximum and minimum limits $\overline{P}_d$ and $\underline{P}_d$. (29) limits the maximum time of DR participation. $\Gamma_{d,m,j}$is the binary indicator for ILDR participation and $\hbar$ is an integer. (30) and (31) give the participation of SLDR through load reduction and increment, respectively for different services. (32) restricts simultaneous decrement and increment of load d' at interval m. The net energy through SLDR is maintained zero (32). $P^{s+}_{d',m,j}$ and $P^{s-}_{d',m,j}$ indicate electricity demand reduction and increment to virtually increase/decrease electricity generation, respectively.

$$P^{s}_{d,m,j} + P^{\delta}_{d,m,j} + \alpha^{u}_{d,m,j} + \ell_{d,m,j} + f^{u}_{d,m,j} \leq \overline{P}_d \Gamma_{d,m,j} \tag{27}$$

$$P^{s}_{d,m,j} - P^{\delta}_{d,m,j} - \ell_{d,m,j} \geq \underline{P}_d \Gamma_{d,m,j} \tag{28}$$

$$\sum_{m}^{M} \Gamma_{d,m,j} \leq \hbar \tag{29}$$

$$0 \leq P^{s+}_{d',m,j} + P^{\delta+}_{d',m,j} + \alpha^{u}_{d',m,j} + \ell_{d',m,j} + f^{u}_{d',m,j} \leq \overline{P}_{d'} \Upsilon_{d',m,j} \tag{30}$$

$$-\overline{P}_{d'} \Upsilon'_{d',m,j} \leq P^{s-}_{d',m,j} + P^{\delta-}_{d',m,j} + \alpha^{d}_{d',m,j} + f^{d}_{d',m,j} \leq 0 \tag{31}$$

$$\Upsilon_{d',m,j} + \Upsilon'_{d',m,j} \leq 1 \quad , \quad \sum_{m}^{M} (P^{-}_{d',m,j} + P^{+}_{d',m,j}) = 0 \tag{32}$$

3.3.5. Power Flow Constraints

The proposed scheduling problem ensures that power transfer between each bus b and node n is within the technical limits of transmission lines for each scenario. (33) gives power flow in a line. $x_{b,n}$ is the reactance of transmission line connecting bus b with node n. S_{base} is used to convert pu quantity and assumed to be 100 MVA. Constraint (34) ensures that power flow between buses is within line capacity limits $\overline{\varpi}_{b,n}$.

$$\varpi_{b,n,m,j} = (\phi_{b,m,j} - \phi_{n,m,j}) S_{base} / x_{b,n} \quad \forall b, m, j \tag{33}$$

$$-\overline{\varpi}_{b,n} \leq \varpi_{b,n,m,j} \leq \overline{\varpi}_{b,n} \quad \forall b, m, j \tag{34}$$

3.3.6. Power Balance Constraints

Eq. (35) ensures power balance at each node in the optimization at time m under scenario j. Here, D_b, D'_b, E_b, H_b, I_b and N_b are the set of ILDR, SLDR, BESS, PHES, generators, and nodes connected to bus b, respectively. In RT, along with resource schedules, FRP procured from

resources are dispatched for each scenario to meet anticipated netload,

$$\begin{aligned}
&\sum_{i\in I_b}(P^{s/\varphi}_{i,m,j}+f^{u}_{i,m,j}-f^{d}_{i,m,j}+P^{\delta}_{i,m,j})+\sum_{h\in \mathrm{H}_b}(P^{s+/\delta+}_{h,m,j}-P^{s-/\delta-}_{h,m,j}+f^{u}_{h,m,j}-f^{d}_{h,m,j})+\\
&\sum_{e\in E_b}(P^{s+/\delta+}_{e,m,j}-P^{s-/\delta-}_{e,m,j}+f^{u}_{e,m,j}-f^{d}_{e,m,j})+\sum_{d\in D_b}(P^{s}_{d,m,j}+P^{\delta}_{d,m,j}+f^{u}_{d,m,j})+\\
&\sum_{d'\in D'_b}(P^{s+/\delta+}_{d',m,j}+P^{s-/\delta-}_{d',m,j}+f^{u}_{d',m,j}+f^{d}_{d',m,j})+L^{curt}_{b,m,j}-N_{b,m,j}=\sum_{n\in N_b}\varpi_{b,n,m,j}\quad \forall b,m,j
\end{aligned} \tag{35}$$

Power and energy requirements in the stochastic SCED framework are taken from 5-minute temporal real-time netload forecast and associated uncertainty characterization presented in Sections 3.4 and 3.5, respectively.

3.4. Netload Forecasting

LSTM approach is used in the proposed work to forecast real-time netload. Its architecture consists of a set of recurrently connected subnets, termed as, memory blocks. Each memory block contains one or more self-connected memory cells and three multiplicative units - the input, output and forget gates; along with a Recursive Neural Network (RNN) block. These facilitate to write, read and reset cells' operations. A set of equations are modeled to activate forward pass gradient calculation of LSTM hidden layer. The ι, ϕ, ω denote input, forget and output gates, respectively. c refers to one of the C memory cells. w_{xy} represents the weight of the connection from unit x and y. The weights from cell c to various gates are denoted by $w_{c\vartheta}$, where $\vartheta \in [\iota, \phi, \omega]$. $a_{\vartheta t}$ represents the network input to unit ϑ at time t, and activation of unit ϑ at time t is denoted by $b_{\vartheta t}$. s_{ct} defines the state of the cell c at time t. f_ϑ is the activation function of the gates. LSTM architecture is illustrated in Fig. 2 for a single cell. In case of a single input, $a_{\vartheta t} = x_{it}$. The concatenated expressions after each activation function can be denoted as $b_{\vartheta,t} = f_\vartheta(w_{c\vartheta}[h_{t-1}, a_{\vartheta t}]) + \gamma_\vartheta$ and output of each cell is $h_t = f_\omega \tanh(S_t)$

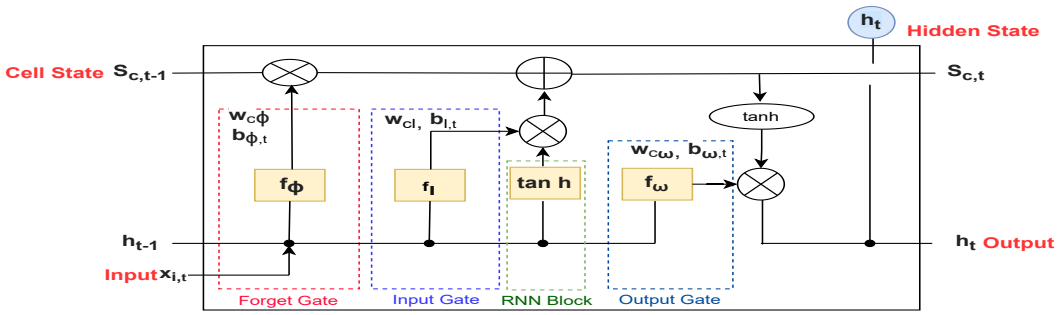

Figure 2: LSTM architecture

The outputs of cell are connected to other blocks in the layer. The activation of states, cell inputs, gates are only visible within the block. i and h denotes the cell's input and hidden layer's output, respectively. LSTM contains more input as compared to output. The forward pass is calculated for a length T sequence by starting at the time $t = 1$ and recursively applying the updates while incrementing. The final weights derivative can be found by summing over the

derivatives at each time step. Equations (36) and (37) define different gates of LSTM [30].

$$a_{\vartheta t} = \sum_{i=1}^{I} w_{i\vartheta} x_{it} + \sum_{h=1}^{H} w_{h\vartheta} b_{h,t-1} + \sum_{c=1}^{C} w_{c\vartheta} s_{c,t-1} \quad \forall \vartheta \in [\iota, \phi, \omega] \tag{36}$$

$$b_{\vartheta t} = f\left(a_{\vartheta t}\right) \quad \forall \vartheta \in [\iota, \phi, \omega] \tag{37}$$

The proposed forecasting model is implemented using Python. Fig. 3 illustrates the step-wise procedure for the process [31]. The studies are conducted on four representative days, $Q1$-$Q4$, one each from four seasons. Historic 5-minute granular data of load, wind, and solar generation of each season is used to estimate netload. This time series is given as input to the model and processed for its use. This includes – data normalization, conversion to supervised time series, segregation of data into train and test data sets. Considering the architecture of LSTM layers, the data is converted into three-dimension. Here, one sequence is equivalent to one sample, one-time step equals a point of observation in the sample, and one feature is one observation at a time step. A single-layer LSTM model is considered with a sigmoid activation function for forget, input, and output gates and tanh for RNN block. The model is compiled by defining *adam* as an optimization algorithm and the *Mean Squared Error (MSE)* as the loss function. Based on the input and output matrix, weights are adjusted to better fit the model. This model is used to predict the netload profile of all representative days, $Q1$-$Q4$.

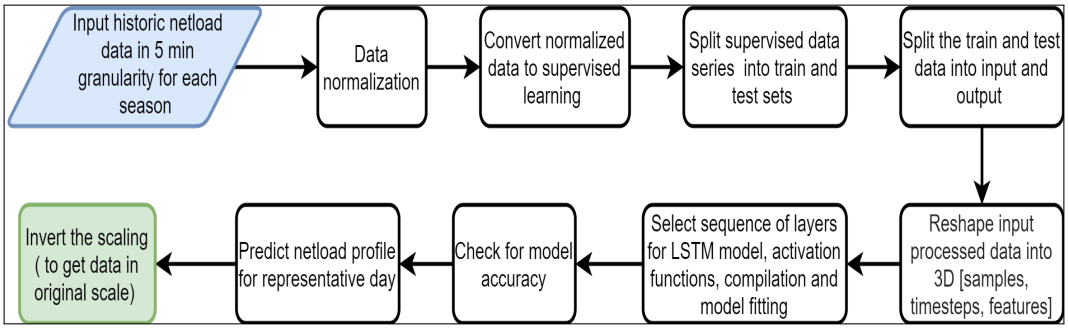

Figure 3: Netload forecasting procedure

3.5. Netload Uncertainty

Netload uncertainty is considered to analyze the impact of netload forecast uncertainties. Netload uncertainty is estimated using MCMC technique. MCMC is a sampling method to characterize distribution without complete mathematical properties by randomly sampling values from the distribution. MCMC methods are widely used in diverse fields to predict the posterior distribution in Bayesian inference. The prime component of this method is Markov Chain that performs a random walk in the search space and consequently reaches the solution. N-Metropolis method is adopted for this work. Netload scenarios are generated from MCMC based multi linear regression using historical data, given in (38) [32, 33],

$$\begin{aligned} Y_h = \beta_0 + \beta_1 X_h + \beta_2 X_h^1 + \beta_3 X_h^2 + \in_h, \in_h \\ = N(0, \sigma^2), h = 1...H \end{aligned} \tag{38}$$

where,Y_h, is the forecasted netload profile of scheduling day and X_h, X_h^1 & X_h^2 are historical netload profiles of previous three days. β_0, β_1, β_2 & β_3 are regression coefficients and $\in_h$ is an observational error. Posterior distribution of model parameters β_0, β_1, β_2 & β_3 can be obtained using likelihood function and prior distribution as follows [33]

$$P(\beta_0, \beta_1, \beta_2, \beta_3, \sigma^2 | y, x) \quad \alpha \quad \left(\frac{1}{\sigma^2}\right)^{\left(\frac{H}{2}\right)+1} e^{\left\{\frac{-1}{2\sigma^2} \sum_{h=1}^{H} [y_h - (\beta_0 + \beta_1 x_h + \beta_2 x_h^1 + \beta_3 x_h^2)]^2\right\}} \tag{39}$$

4. Case Study

4.1. Data and Assumptions

Effectiveness of the proposed methodology is analyzed on IEEE RTS 24 and reduced Great Britain (GB) test systems with a peak demand of 2.7 GW and 70 GW, respectively. Four representative days, $Q1$ - $Q4$, one day from each quarter of a year are examined to investigate the impact of netload seasonal variability on flexibility requirement. Studies are carried out for 30% - 50% RES integration levels. Historical data of load, solar irradiance, and wind speed of California and GB are taken from [34, 35]. Fig. 4 shows 15-minute temporal netload variation for each representative day of both test systems at 30% RES integration. RT forecasting and associated uncertainty characterization are carried out using 5-minute temporal netload time series data. For each representative day, historical netload time series of the corresponding season is used to train and test LSTM model. Fig. 5 compares actual and predicted 5-minute temporal netload profiles of GB system for all representative days at 40% RES. The prediction accuracy is found to be very high. In order to characterize uncertainty in netload forecast, 1000 netload scenarios are generated from β_0, β_1, β_2, β_3 & σ^2 samples using (38). Statistical tool - SAS is used for scenario generation. Table 1 gives the posterior distribution summaries of GB test system for $Q3$ and 30% RES integration. Further, generated scenarios are reduced to 10 plausible sets to reduce the computational burden. Reduced scenarios and associated probabilities are obtained from the backward scenario reduction method, implemented using SCENRED2 in GAMS 24.2.3.

Figs. 6a and 6b present the reduced netload scenarios of both test systems for $Q4$ and 30% RES integration. Due to larger time intervals, the granularity of randomly selected portions is highlighted in upper part of the figures. Statistical properties of these highlighted portions are shown in Figs. 7a and 7b for corresponding systems. The average difference between mean and standard deviations of generated and reduced scenarios is found to be less than 1% and 7%, respectively. This justifies the proficiency of scenario reduction method as scenario distribution of both generated and reduced scenarios is identical.

PHES of 200 MW capacity having 08 hours discharge time with a reservoir (upper and lower) capacity of 1 TMC, and a 50 MW/200 MWh BESS are considered [36, 37]. The maximum capacity of ILDR and SLDR is assumed to be 10% of peak load at each bus. Up/down regulation requirement is assumed to be 1% of load at time m. Spinning reserves are allocated by approximating their full deployment in 10-minutes from the time of contingency. Netload uncertainty components for FRP estimation are calculated from the standard deviation of historical netload data at 95% confidence interval. The proposed MILP is formulated in GAMS 24.2.3 and solved using CPLEX solver on 3.4 GHz, Intel i7 processor with 16 GB RAM. All simulations for RT-SCED are solved under 300 seconds.

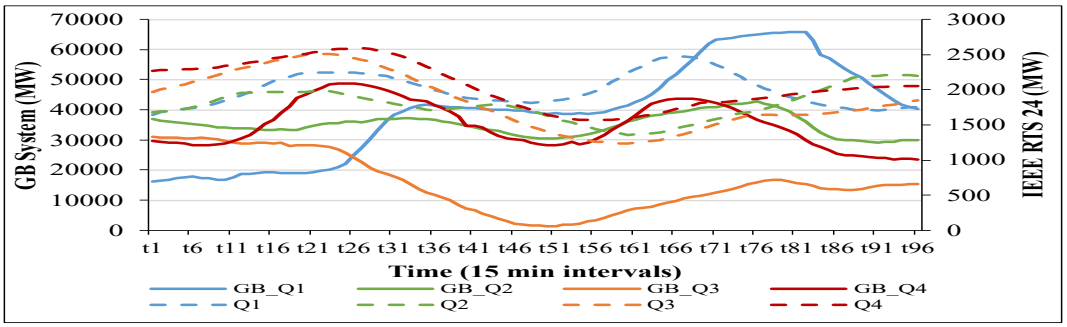

Figure 4: Seasonal netload

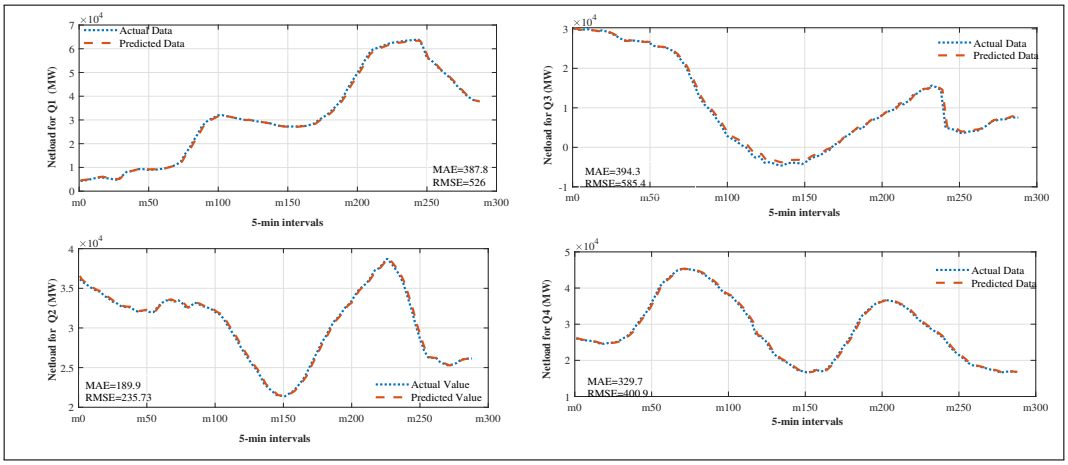

Figure 5: Forecasted netload profiles for GB test system

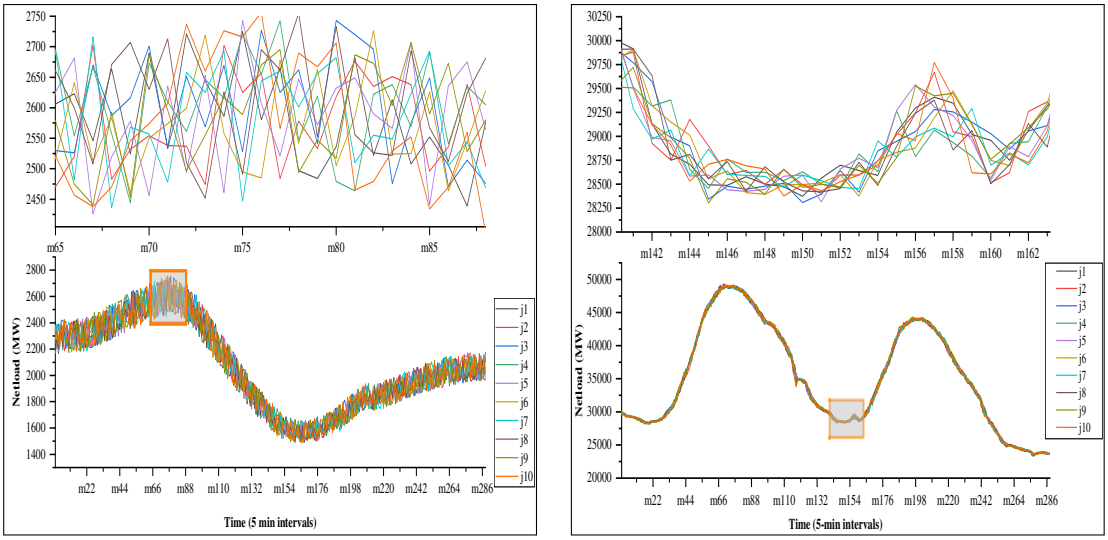

(a) IEEE RTS

(b) GB system

Figure 6: Reduced Netload Scenarios

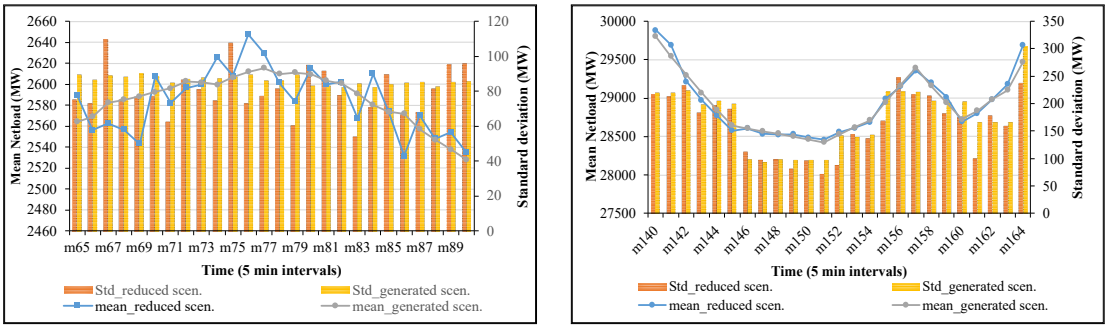

(a) IEEE RTS (b) GB system

Figure 7: Statistical properties of generated and reduced netload scenarios

Table 1: Posterior summaries and intervals of MCMC

Parameter	N	Mean	Std. deviation	95% HPD interval	
$\beta 0$	1000	3617.9	3.7056	3613.3	3625.1
$\beta 1$	1000	-1.8174	0.000456	-1.8186	-1.8169
$\beta 2$	1000	-1.1877	0.000385	-1.1883	-1.1869
$\beta 3$	1000	3.4628	0.000259	3.4624	3.4631
σ^2	1000	17.0947	0.000347	17.094	17.0954
Sampling method		N-metropolis	Shape factor	3/10	
			Scale factor	10/3	

4.2. IEEE RTS 24

4.2.1. Case-1: Impact of Increasing RES Integration

Increasing RES integration from 30%-50% has decreased operating costs for all representative days, $Q1-Q4$, in DA scheduling. However, diverse pattern in operating cost is observed in RT with netload uncertainty consideration. Variation in operating cost is primarily due to load curtailment caused by ramp insufficiency of scheduled resources. Although additional scheduling of committed resources significantly reduced inflexibility, maximum ramp-up insufficiency of 153 MW is observed for $Q4$ at 30% RES integration. Total power insufficiency of 5-minute dispatch intervals is 3813 MW for $Q4$ at 30% RES and energy insufficiency is 318 MWh. RT up/ down capacity of 702 MWh and 716 MWh is additionally dispatched for $Q4$ and $Q1$ at 30% RES, respectively.

4.2.2. Case-2: Impact of Flexible Resources Integration

Integrating flexible resources like BESS, PHES, ILDR, and SLDR has shown a significant improvement in operating costs and technical parameters for all representative days and integration levels compared to Case-1. Similar to Case-1, RT operating costs tend to increase from 50% RES integration for $Q1$ and $Q4$. Whereas operating costs reduced with increasing RES integration in $Q2$ and $Q3$. A maximum reduction in RT operating cost of 15.98% is observed for $Q4$ at 40% RES. Flexible resources integration has reduced magnitude and frequency of inflexibility events for all representative days and RES integration levels compared to Case-1. Further, in comparison to the scenario presented in Case-1, maximum ramp insufficiency for $Q4$ has reduced 7.85% in the case

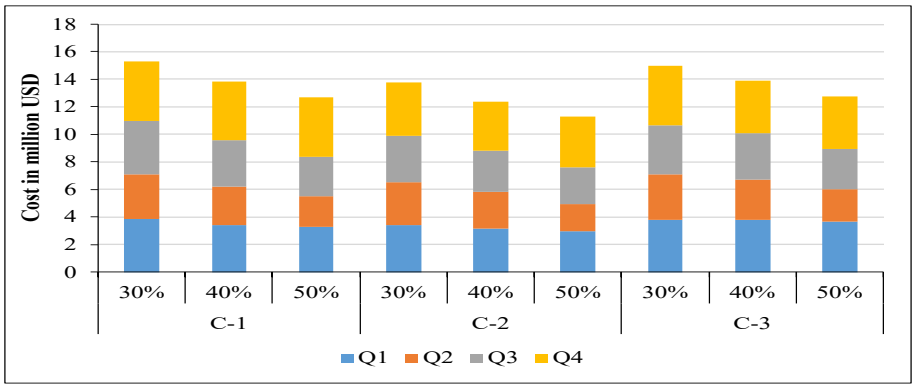

Figure 8: Operating cost comparison for IEEE RTS 24

at 30% RES. Total power insufficiency of 5-minute dispatch intervals and total energy insufficiency reduced to 2262 MW and 189 MWh for $Q4$ and 30% RES. Also, integration of flexible resources increased the residual capacity of committed resources and a slight increment in its utilization is observed in all representative days. A maximum additional capacity of 1000 MWh is scheduled for $Q3$ at 30% RES and a maximum ramp down capacity of 749 MWh is utilized in $Q4$ and 40% RES.

4.2.3. Case-3: Impact of Integrating Flexible Ramp Products

To ensure sufficient ramping availability in RT, many ISOs are implementing new market products, termed, Flexible Ramp Products (FRPs). These FRPs secure additional ramping from eligible resources and dispatch them in RT. In this case, FRPs are integrated with the system outlined in Case-2. FRPs are secured in DA scheduling by co-optimizing with energy and ancillary services. Integrating ramp products has increased operating costs compared to other cases due to additional capacity requirement for FRP provision. However, a significant reduction in penalties and improvement in the system's netload uncertainty handling capability is observed with the utilization of FRPs. Average ramp insufficiency reduction of 44.3% for all integration levels and representative days with a maximum reduction of 88% for $Q1$ at 30% RES in comparison to Case-1 is observed. In comparison to Cases-1 and 2, total power insufficiency for $Q4$ at 30% RES is reduced to 1116 MW and associated energy insufficiency to 93 MWh. Around 50% reduction in the dependency on additional scheduling of resources is noticed for all representative days and integration levels.

Fig. 8 illustrates the total operating cost for all cases. System operating costs tend to vary from $Q1$ to $Q4$ due to seasonal netload variability. RT operating costs decreased 35.6% and 18.22% with FRP integration compared to Cases-1 and 2, respectively. However, total operating cost in this case is more due to increase in DA scheduling cost. DA operating costs increased 13.52% and 20.92% in Case-3 as compared to Cases 1 and 2. Also, total operating cost of all cases tends to decrease with increasing RES integration.

4.2.4. Flexibility Indices

MUT/MDT, start up and shut down times play an important role in DA scheduling. As the simulation is carried out in a multi-interval time frame and fast-start resources are scheduled based on their operating status and technical constraints, resources operating range and ramping limits can sufficiently estimate flexibility. RFI presented in (5) and (6) are integrated with the scheduling framework to evaluate the flexibility scores. These indices highlight the flexibility contribution

of individual resources for the scheduling day. OR index near zero for more units highlights the inflexibility in MSG or ramp down in the system. Similarly, the value near one indicates the possibility of ramp-up insufficiency during contingencies. Ramping index near zero highlights the system's incapability of utilizing the available ramping from resources. Figs. 9a, 9b and 9d give the mean scores for individual and combined RFI of all representative days, $Q1 - Q4$, at 30% RES integration. An equal weight of 0.5 is assumed for calculating combined RFI from OR and ramping *i.e.*, $CRFI_\chi = 0.5RFI_\chi^{OR} + 0.5RFI_\chi^{ramp}$

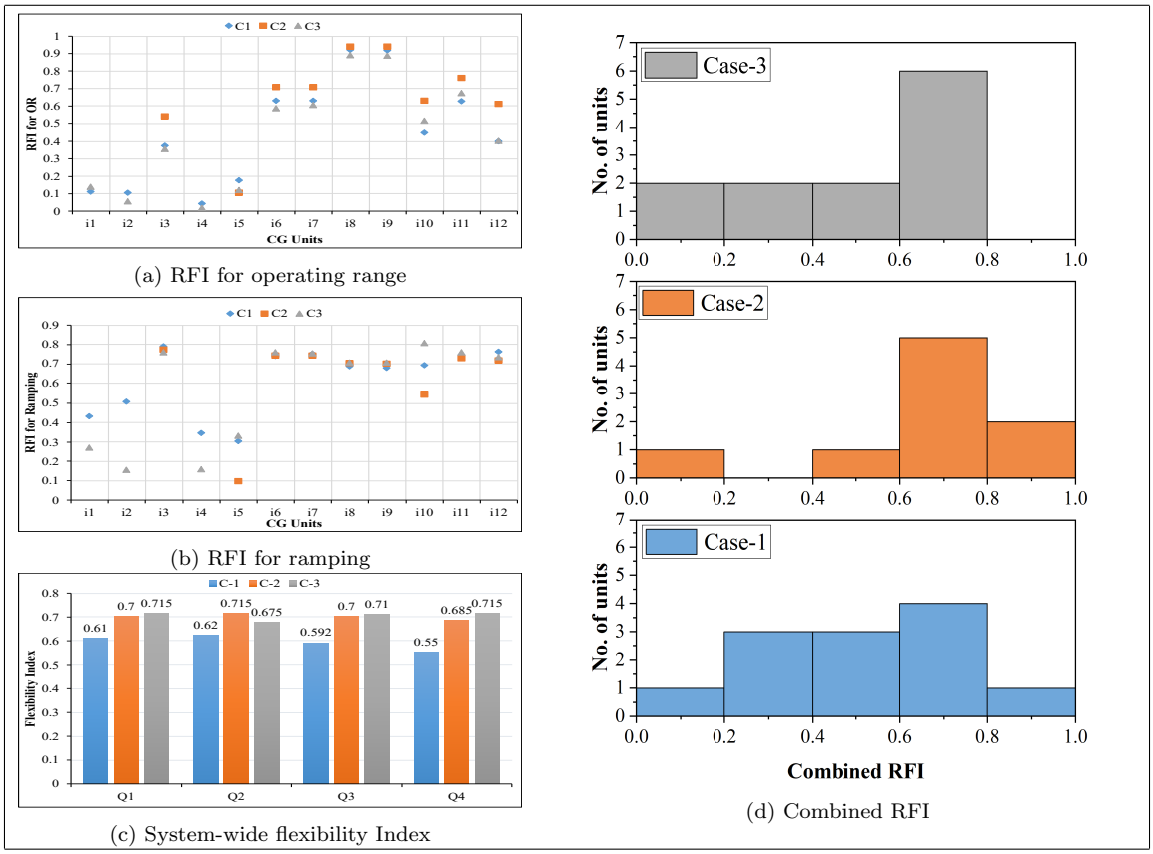

(a) RFI for operating range

(b) RFI for ramping

(c) System-wide flexibility Index

(d) Combined RFI

Figure 9: Mean flexibility index of cases at 30% RES for IEEE RTS 24

Fig. 9a illustrates the flexibility index of generating units for OR. In Case-1, when only CG units are available, the RFI for maximum units is near zero. This is due to the generating units turned ON to meet demand at few intervals are scheduled to operate near MSG to fulfill their MUT. However, improvement in the index is observed with the integration of flexible resources or FRPs as given in Cases-2 and 3. Fig. 9b highlights resource flexibility in terms of ramping. Higher value of this index gives resources ramp availability. The combined flexibility index of the cases for $Q1$ and 30% RES is given in Fig. 9d. A reduction in the number of committed CG units is observed due to improvement in flexibility with the integration of flexible resources and FRPs. More number of units operating at higher combined RFI denote higher flexibility. Similar trend is observed for all representative days and RES integration levels. System-wide flexibility can be obtained upon integrating and normalizing resources in the combined flexibility index, $\sum_\chi CRFI_\chi$. Higher the value of system flexibility index, the greater is the flexibility of the system. Fig. 9c gives

the system flexibility index for $Q1-Q4$ at 30% RES. Higher flexibility index in each representative day indicates greater flexibility in handling netload uncertainty and vice-versa. A high flexibility index (0.715) in Case-3 and $Q1$ indicates the mitigation of a large amount of ramp and power insufficiency events, with maximum ramp insufficiency reduced to 4.2% of peak load. Table 2 gives the technical comparison of cases for $Q4$ at 50%.

Table 2: Technical comparison of cases for IEEE RTS 24

	C-1	C-2	C-3
DA Operating cost ($M)	3.43	3.02	3.37
RT operating cost ($M)	0.87	0.63	0.45
Maximum Ramp insufficiency (MW/5min)	140.26	130.24	102.56
Total power insufficiency (MW)	3732	2670	1900
Total Energy insufficiency (MWh)	311	222.5	158.33
Energy up schedule (MWh)	678.91	833.33	581.58
Energy down schedule (MWh)	570.83	676	362.25
FRU(MWh)	0	0	560.66
FRD(MWh)	0	0	382
System flexibility index	0.64	0.7	0.72
DA Computational time (secs)	930	1200	1535
Number of startups /shutdowns	10/13	8/12	3/7
Average load factor	53.4	48.50	50.86

4.2.5. Impact of Minimum Stable Generation on RFI

Further, to analyze the impact of MSG on RFI, CG units are scheduled at 40% technical minimum. Reduction in operating cost and inflexibility are observed at 40% MSG compared to the case with CG units operation at 50% MSG. Fig. 10 gives the comparison of RFI for Case-1 at 50% and 40% MSG (T50% and T40%) for IEEE RTS 24. Results further justify the discussion on Fig. 9a. Decreasing MSG resulted improvement in units' OR, which further reduced the non-essential start up of units. This resulted in RFI score improvement for most of the generators.

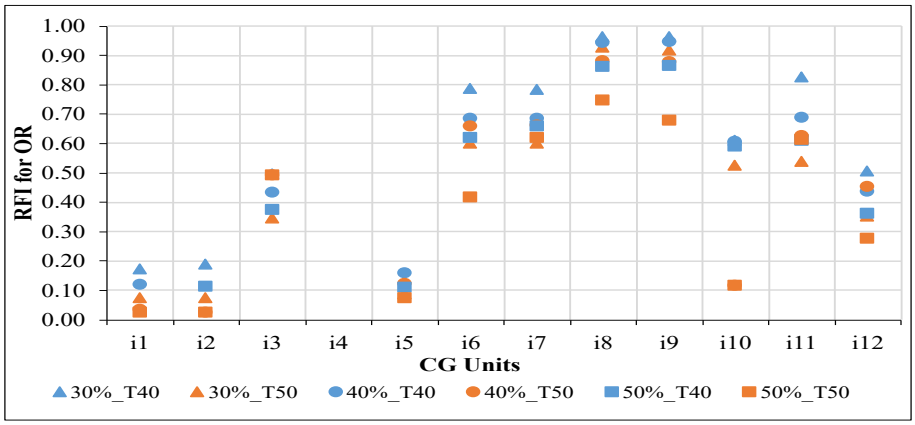

Figure 10: RFI comparison for 40% and 50% MSG

4.3. Reduced GB Test system

Similar case studies are carried out on reduced GB test system to validate the scalability of proposed work. Increasing RES integration resulted in the reduction of DA operating cost for all representative days except $Q3$. Operating costs tend to increase from 30% - 40% and decrease for 50% RES integration in $Q3$, due to high renewable curtailment. RT operating costs varied in all cases due to netload uncertainty. However, system's total operating cost reduced with increasing RES integration. Fig. 11 gives operating costs of all cases at various RES integration levels.

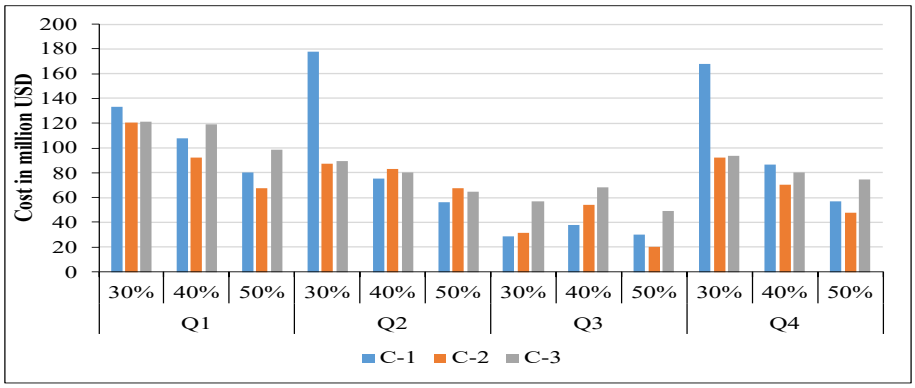

Figure 11: Operating cost comparison for reduced GB test system

A higher system inflexibility in handling RT netload uncertainty is observed in the base case *i.e.,* Case-1. A maximum ramp insufficiency of 6513 MW is observed for $Q4$ at 30% RES. RT up/ down capacity of 3700 MWh and 10 GWh is additionally scheduled. Total power insufficiency of 5-minute dispatch intervals is 465808 MW for $Q4$ at 30% RES and associated energy insufficiency is 38 GWh for whole day scheduling. Utilizing flexible resources significantly reduces inflexibility events. The magnitude of ramp insufficiency reduced to 1538 MW for $Q4$ at 30% RES. Total power insufficiency reduced to 14145 MW and corresponding energy insufficiency to 1.18 GWh. Integrating ramp products has resulted in a significant improvement in system performance with ramp and power insufficiency reduction of 76.38% and 96% as compared to Case-2. Also, 85% and 98% reduction in Ramp and power insufficiency from Case-1 is observed for $Q4$ at 30% RES integration. Figs. 12a, 12b and 12d give mean RFI for generating units. A large number of units are scheduled near $\overline{P}_i$ or at their MSG, $\underline{P}_i$. This highlights inflexibility in MSG and MUT. Fig. 12c gives system-wide flexibility index for all cases. Similar to IEEE RTS -24, cases with higher flexibility index found to have a lower frequency of inflexibility in respective representative days. Table 3 gives technical comparison of cases for $Q4$ at 50% RES.

Although improvement in system-flexibility is observed in Cases- 2 and 3, limited capacity of flexible resources and ramp products resulted in inflexibility events. Planning additional flexible resources along with the integration of FRPs can completely eliminate inflexibility events. Also, in both test systems, a decrement in load factor of CG units' is observed with the integration of flexible resources and decreasing MSG. This highlights the need for compensation mechanism for such units to cater their wear and tear.

5. Conclusion

With the proliferation of variable and uncertain renewable energy sources integration, system operators need to assess flexibility requirements in upcoming scheduling intervals. The paper

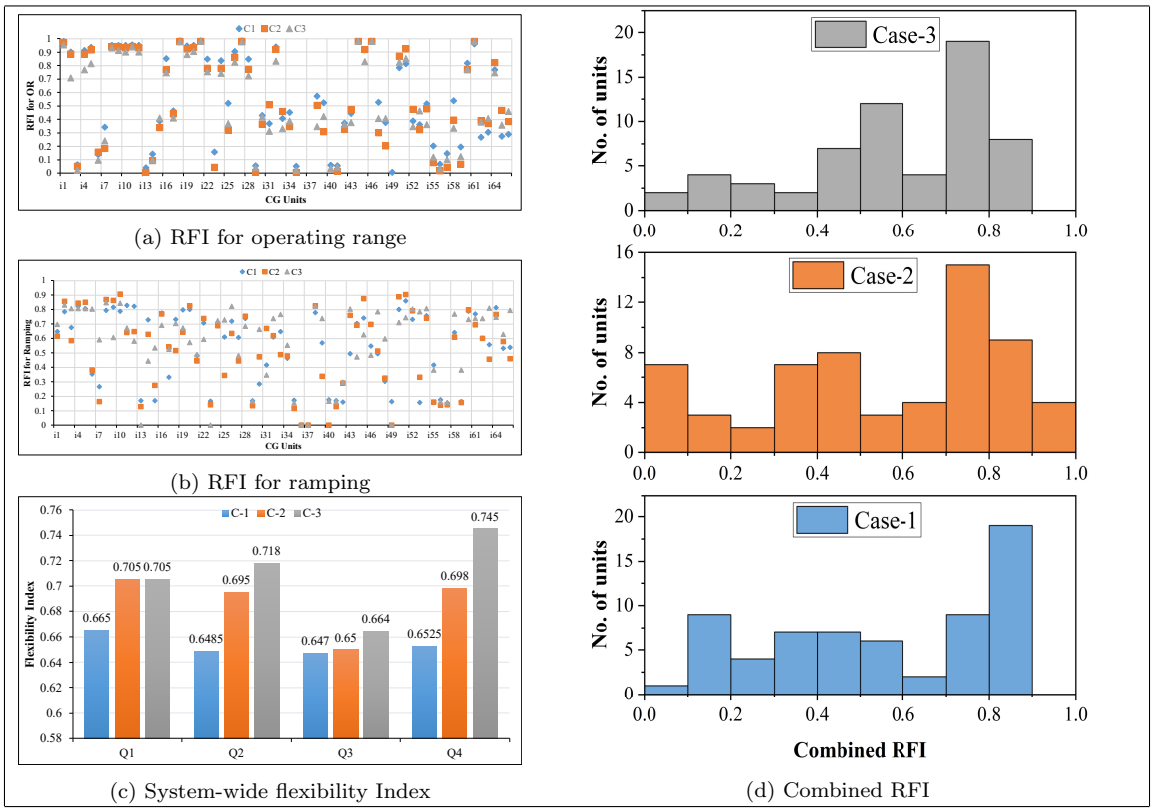

(a) RFI for operating range

(b) RFI for ramping

(c) System-wide flexibility Index

(d) Combined RFI

Figure 12: Mean flexibility index of cases at 30% RES for reduced GB system

Table 3: Technical comparison of cases for reduced GB system

	C-1	C-2	C-3
DA Operating cost ($M)	48.14	45.38	47.62
RT operating cost ($M)	8.63	2.54	0.06
Maximum Ramp insufficiency (GW/5min)	2.94	1.33	0.065
Total power insufficiency (GW)	78.77	17.16	0.072
Total Energy insufficiency (GWh)	6.56	1.43	0.006
Energy up schedule (GWh)	2.83	3.24	0.13
Energy down schedule (GWh)	0.05	0.029	0
FRU (GWh)	0	0	14.36
FRD (GWh)	0	0	5.29
System flexibility index	0.65	0.69	0.8
DA Computational time (secs)	2814	3200	1560
Number of startups /shutdowns	62/98	38/50	28/47
Average load factor	62.80	42.30	55

proposes an explicit framework to assess system-wide flexibility in terms of ramp, power and energy insufficiency. Further, an index to quantify resource flexibility based on operating range and ramping is proposed. The flexibility quantification metric and index are integrated with a stochastic multi-interval scheduling framework. Real-time netload is forecasted using Long Short-Term Memory. Netload uncertainty associated with the forecast is quantified using scenarios

derived from the Markov Chain Monte Carlo technique. Following observations are made from the case studies –

- The proposed framework effectively quantifies system inflexibility in terms of ramp, power, and energy insufficiency. Also, the value of resource flexibility index in each case is found to be proportional to system's netload variability handling capability.
- Integrating demand response and energy storage systems improves flexibility at a lower cost compared to utilizing conventional generation.
- Ramp products can significantly improve flexibility, however with some increased operating cost.
- Reducing minimum stable generation of conventional generators has exploited additional operational flexibility.
- Average inflexibility can be reduced up to 97% with the utilization of emerging resources and ramp products.

The proposed methodology can be extended to consider the coordinated operation of interconnected systems to enhance flexibility and assess their impact on the metric. The proposed scheduling framework can be improved by including multiple intraday netload updations for the accurate estimation of flexibility requirements. Analysis of techno-economic impact on resources flexibility provision can help system operators in taking appropriate control actions. Although the work considers various flexible resources, emerging resources like electric vehicles and virtual storage can also be integrated with the proposed scheduling framework.

6. Acknowledgment

This work has been conducted as a part of the research projects 'UK India Clean Energy Research Institute (UKICERI)', funded by Department of Science and Technology - India (Grant No. DST/RCUK/JVCCE/2015/02) and 'Joint UK-India Clean Energy Centre (JUICE)' funded by the RCUK's Energy Programme (contract no: EP/P003605/1).

Appendix A. Day Ahead - Security Constrained Unit Commitment

Notations for variables represent the same as in RT, however with 15-minute time intervals, t.

$$Obj = min\ (\lambda_{En}^{DA} + \lambda_{\alpha}^{DA} + \lambda_{\ell}^{DA} + \lambda_{f}^{DA} + \lambda^{RC}) \tag{A.1}$$

$$\begin{aligned}\lambda_{En}^{DA} = &\sum_{i,t}\left[(C_i^{\min} u_{i,t} + \sum_k Sl_{i,k} P_{i,k,t}^{s}) + (C_i^{st} y_{i,t} + C_i^{sd} z_{i,t})\right] + \sum_{e,t} C_e P_{e,t}^{s-} \\ &\sum_{h,t}\left[C_h^{+} P_{h,t}^{s+} + C_h^{-} P_{h,t}^{s-}\right] + \sum_{d/d',t} C_d\left[P_{d,t}^{s} + P_{d',t}^{s+}\right]\end{aligned} \tag{A.2}$$

$$\lambda_{\alpha}^{DA} = \sum_{\chi,t} C^{\alpha}\left[\alpha_{\chi,t}^{u} + \alpha_{\chi,t}^{d}\right] + \sum_{d,t} C^{\alpha}\alpha_{d,t}^{u} \quad \forall \chi \in [D', E, H, I] \tag{A.3}$$

$$\lambda_{\ell}^{DA} = \sum_{\chi,t} C^{\ell} \ell_{\chi,t} \quad \forall \chi \in [D, D', E, H, I] \tag{A.4}$$

$$\lambda_{f}^{DA} = \sum_{\chi,t} C^{f} \left[f_{\chi,t}^{u} + f_{\chi,t}^{d} \right] + \sum_{d,t} C^{f} f_{d,t}^{u} \quad \forall \chi \in [D', E, H, I] \tag{A.5}$$

$$\lambda^{RC} = C^{curt} \left[\sum_{s,t} P_{s,t}^{sc} + \sum_{w,t} P_{w,t}^{wc} \right] \tag{A.6}$$

Eq. (A.1) gives the objective function of the proposed Day-Ahead Security Constrained Unit Commitment (DA- SCUC). The SCUC is solved to minimize the total operating cost incurred for cost of electricity generation (λ_{En}^{DA}), allocating regulation (λ_{α}^{DA}), reserve (λ_{ℓ}^{DA}) and FRP (λ_{f}^{DA}) along with renewable curtailment (λ^{RC}). Eq. (A.2) gives the cost of electricity generation from CG units and flexible resources. First term of (A.2) gives the linearized cost function of CG units along with its cost for minimum generation and start up/shutdown [38]. $u_{i,t}$, $y_{i,t}$ and $z_{i,t}$ are the binary variables representing unit's running, start and shutdown status. Second term of (A.2) represents the charging cost of BESS, where C_e is the charging cost per MW. Third term of (A.2) highlights the cost of power generated and consumed in generating and motoring modes of PHES. C_h^+ , C_h^- and $P_{h,t}^{s+}$, $P_{h,t}^{s-}$ are the costs and scheduled power in generating and motoring modes. Last part of (A.2) denotes cost incurred in utilizing interruptible and time shifting demand response schemes. $P_{d,t}^{s}$ is the utilized capacity of ILDR and $P_{d,t}^{s+}/P_{d,t}^{s-}$ is power decrement/increment from SLDR. (A.3)-(A.5) gives total cost incurred for securing up and down regulation ($\alpha_{\chi,t}^{u/d}$), reserve ($\ell_{\chi,t}$) and flexible ramp product ($f_{\chi,t}^{u/d}$) services from resources. $C^{\alpha/\ell/f}$ are the offer prices for regulation, reserve and FRP, respectively. (A.6) highlights the penalty for solar and wind power curtailment.

$$P_{i,t}^{s} + \alpha_{i,t}^{u} + \ell_{i,t} + f_{i,t}^{u} \leq \bar{P}_i u_{i,t} \quad \forall i, t \tag{A.7}$$

$$P_{i,t}^{s} - \alpha_{i,t}^{d} - \ell_{i,t} - f_{i,t}^{d} \geq \underline{P}_i u_{i,t} \quad i, t \tag{A.8}$$

$$P_{i,t}^{s} - P_{i,t-1}^{s} + \alpha_{i,t}^{u} + \ell_{i,t} + f_{i,t}^{u} + f_{i,t-1}^{d} \leq \tau\, r_i^{u}\, u_{i,t-1} + \tau\, r_i^{st}\, y_{i,t} \quad \forall i, t \tag{A.9}$$

$$P_{i,t-1}^{s} - P_{i,t}^{s} + \alpha_{i,t}^{d} + f_{i,t}^{d} + f_{i,t-1}^{u} \leq \tau\, r_i^{d} u_{i,t} + \tau\, r_i^{sd} z_{i,t} \quad \forall i, t \tag{A.10}$$

$$\alpha_{i,t}^{u} + \ell_{i,t} \leq \xi' r_i^{u} \quad , \quad \alpha_{i,t}^{d} \leq \xi' r_i^{d} \tag{A.11}$$

$$f_{i,t}^{u} \leq \xi r_i^{u} \quad , \quad f_{i,t}^{d} \leq \xi r_i^{d} \tag{A.12}$$

Constraints (A.7)-(A.12) give the operating constraints of CG units. (A.7) and (A.8) ensure that the total power generation for energy and ancillary services do not violate respective unit's operating range. Ramping limitations on CG units scheduling is denoted using (A.9) and (A.10). Here, $\tau = 3$ is used to estimate ramping in 15-minute temporal. Constraints (A.11) and (A.12) ensure that the ancillary services dispatch-ability is as per market regulations. ξ and ξ' are 3 and

2, respectively.

$$SOC_{e,t} = SOC_{e,t-1} + [P^{ch}_{e,t}\eta^{ch}_{e} - P^{di}_{e,t}/\eta^{di}_{e}]\Delta t \quad \forall e,t \tag{A.13}$$

$$\underline{SOC}_e \leq SOC_{e,t} \leq \overline{SOC}_e \qquad \forall t \tag{A.14}$$

$$P^{s-}_{e,t} + \alpha^{d}_{e,t} + f^{d}_{e,t} \leq \bar{P}^{ch}_{e}\psi_{e,t} \quad \forall t \tag{A.15}$$

$$P^{s+}_{e,t} + \alpha^{u}_{e,t} + \ell_{e,t} + f^{u}_{e,t} \leq \bar{P}^{di}_{e}\zeta_{e,t} \quad \forall t \tag{A.16}$$

$$P^{s-}_{e,t} \geq \underline{P}^{ch}_{e}\psi_{e,t} \quad , \quad P^{s+}_{e,t} \geq \underline{P}^{di}_{e}\zeta_{e,t} \quad \forall t \tag{A.17}$$

$$\psi_{e,t} + \zeta_{e,t} \leq 1 \quad \forall t \tag{A.18}$$

SOC at the end of current scheduling interval depends on its level in previous interval, total discharging ($P^{di}_{e,t}$) and charging ($P^{ch}_{e,t}$) power of BESS in current interval, as shown in (A.13). To avoid deep discharge of BESS, the SOC is limited within an optimal range as represented by (A.14). (A.15), (A.16) and (A.17) ensure BESS power allocation for various services is within its maximum and minimum rated dis/charging capability. (A.18) limits BESS from its simultaneous participation in charging and discharging, where $\psi_{e,t}$ and $\zeta_{e,t}$ are binary variables representing charging and discharging modes. ($P^{di}_{e,t}$) and ($P^{ch}_{e,t}$) is the sum of allocated power for energy and ancillary services in discharging and charging modes, respectively.

$$P^{prod}_{h,t} = (\eta^{G}_{h}\rho g H^{UR})Q^{+}_{h,t} \tag{A.19}$$

$$P^{cons}_{h,t} = (\rho g H^{LR})Q^{M}_{h,t}/\eta^{M}_{h} \tag{A.20}$$

$$L^{UR}_{h,t} = L^{UR}_{h,t-1} + (Q^{-}_{h,t} - Q^{+}_{h,t})t \tag{A.21}$$

$$L^{LR}_{h,t} = L^{LR}_{h,t-1} + (Q^{+}_{h,t} - Q^{-}_{h,t})t \tag{A.22}$$

$$P^{s+}_{h,t} + \alpha^{u}_{h,t} + \ell_{h,t} + f^{u}_{h,t} \leq P^{prod}_{h,t} \tag{A.23}$$

$$P^{s-}_{h,t} + \alpha^{d}_{h,t} + f^{d}_{h,t} \leq P^{cons}_{h,t} \tag{A.24}$$

Unlike BESS, generated and consumed power of PHES are constrained by the head of upper and lower reservoirs (H^{UR}/H^{LR}), water discharge between the reservoirs in generating and motoring modes $Q^{+/-}_{h,t}$ along with the operational efficiencies ($\eta^{G/M}_{h,t}$) in generating and motoring modes, respectively. (A.19) and (A.20) give the relation among various parameters in power generation and motoring modes of PHES. P^{prod} / P^{cons} are the total power produced /consumed in generating and motoring modes. (A.21) and (A.22) depict the water level of upper and lower reservoirs, which depend on water flow at the current scheduling interval and water level of reservoirs at the previous

interval. The levels are inversely related to each other. (A.23) and (A.24) give the power allocation of various services.

DA constraints of ILDR and SLDR holds the same as given in (27)-(32) of Section 3, however $\forall t$

$$N_{b,t} = L_{b,t} - \sum_{s \in S_b} P_{s,t} - \sum_{w \in W_b} P_{w,t} \quad \forall b, t \tag{A.25}$$

$$\sum_{i \in I_b} P_{i,t} + \sum_{h \in \mathrm{H}_b} (P^{+}_{h,t} - P^{-}_{h,t}) + \sum_{e \in E_b} (P^{+}_{e,t} - P^{-}_{e,t}) + \sum_{d \in D_b} P_{d,t} + \sum_{d' \in D'_b} (P^{+}_{d',t} + P^{-}_{d',t}) - N_{b,t} = \sum_{n \in B_b} \varpi_{b,n,t} \quad \forall t \tag{A.26}$$

Netload at each bus $N_{b,t}$ is the difference between load $L_{b,t}$ and solar and wind generation $P_{s,t}$, $P_{w,t}$ integrated to the bus b , as given in (A.25). In DA scheduling resources are dispatched to meet 100% of anticipated load. However, it results in some renewable power curtailment, $P^{sc}_{s,t}$ and $P^{wc}_{w,t}$, which is limited by a high penalty for curtailment. (A.26) ensures the power balance at each bus b and time t. $\varpi_{b,n,t}$ is the power flow between bus b and node n. Transmission line security limits are ensured using the constraints as given in (33) and (34) of Section 3, $\forall t$. Sum of allocated reserve, regulation and FRP are equal to their respective requirements.

References

[1] H. Nosair, F. Bouffard, Flexibility envelopes for power system operational planning, IEEE Trans. Sustain. Energy 6 (3) (2015) 800–809.

[2] O. Agbonaye, P. Keatley, Y. Huang, O. O. Ademulegun, N. Hewitt, Mapping demand flexibility: A spatio-temporal assessment of flexibility needs, opportunities and response potential, Appl. Energy 295 (2021) 117015.

[3] M. Z. Degefa, I. B. Sperstad, H. Sæle, Comprehensive classifications and characterizations of power system flexibility resources, Elect. Power Syst. Res. 194 (2021) 107022.

[4] L. Söder, E. Tómasson, A. Estanqueiro, D. Flynn, B.-M. Hodge, J. Kiviluoma, et al., Review of wind generation within adequacy calculations and capacity markets for different power systems, Renew. Sustain. Energy Rev. 119 (2020) 109540.

[5] I. F. Abdin, E. Zio, An integrated framework for operational flexibility assessment in multi-period power system planning with renewable energy production, Appl. Energy 222 (2018) 898–914.

[6] T. Heggarty, J.-Y. Bourmaud, R. Girard, G. Kariniotakis, Multi-temporal assessment of power system flexibility requirement, Appl. Energy 238 (2019) 1327–1336.

[7] K. P. Olsen, Y. Zong, S. You, H. Bindner, M. Koivisto, J. Gea-Bermúdez, Multi-timescale data-driven method identifying flexibility requirements for scenarios with high penetration of renewables, Appl. Energy 264 (2020) 114702.

[8] Y. Dvorkin, D. S. Kirschen, M. A. Ortega-Vazquez, Assessing flexibility requirements in power systems, IET Gen., Trans. & Dist. 8 (11) (2014) 1820–1830.

[9] M. Huber, D. Dimkova, T. Hamacher, Integration of wind and solar power in Europe: Assessment of flexibility requirements, Energy 69 (2014) 236–246.

[10] A. Ulbig, G. Andersson, Analyzing operational flexibility of electric power systems, Int. J. Elect. Power & Energy Systems 72 (2015) 155–164.

[11] Y. Yasuda, A. R. Ardal, E. M. Carlini, A. Estanqueiro, D. Flynn, E. Gomez-Lázaro, et al., Flexibility chart: Evaluation on diversity of flexibility in various areas, 12^{th} Int. Workshop on Large-Scale Integration of Wind Power into Power Systems as well as on Transmission Networks for Offshore Wind Power Plants (2013).

[12] Q. Wang, H. Wu, A. R. Florita, C. B. Martinez-Anido, B. M. Hodge, The value of improved wind power forecasting: Grid flexibility quantification, ramp capability analysis, and impacts of electricity market operation timescales, Appl. Energy 184 (2016) 696–713.

[13] V. Oree, S. Z. S. Hassen, A composite metric for assessing flexibility available in conventional generators of power systems, Appl. Energy 177 (2016) 683–691.

[14] Y.-K. Wu, W.-S. Tan, S.-R. Huang, Y.-S. Chiang, C.-P. Chiu, C.-L. Su, Impact of generation flexibility on the operating costs of the taiwan power system under a high penetration of renewable power, IEEE Trans. Indust. Applications 56 (3) (2020) 2348–2359.
[15] E. Heydarian-Forushani, M. E. H. Golshan, P. Siano, Evaluating the operational flexibility of generation mixture with an innovative techno-economic measure, IEEE Trans. Power Syst. 33 (2) (2017) 2205–2218.
[16] A. Nikoobakht, J. Aghaei, M. Shafie-Khah, J. P. Catalao, Assessing increased flexibility of energy storage and demand response to accommodate a high penetration of renewable energy sources, IEEE Trans. Sustain. Energy 10 (2) (2019) 659–669.
[17] S. Y. Abujarad, M. Mustafa, J. Jamian, A. Abdilahi, Flexibility quantification for thermal power generators using deterministic metric for high renewable energy penetration, 2016 IEEE Int. Conf. on Power and Energy (PECon) (2016) 580–584.
[18] J. Yang, L. Zhang, X. Han, M. Wang, Analysis on operational flexibility and generation reliability in generation schedule, 2016 IEEE Innovative Smart Grid Technologies-Asia (ISGT-Asia) (2016) 642–646.
[19] A. A. Thatte, L. Xie, A metric and market construct of inter-temporal flexibility in time-coupled economic dispatch, IEEE Trans. Power Syst. 31 (5) (2015) 3437–3446.
[20] E. Lannoye, D. Flynn, M. O'Malley, Transmission, variable generation, and power system flexibility, IEEE Trans. Power Syst. 30 (1) (2015) 57–66.
[21] F. Pourahmadi, H. Heidarabadi, S. H. Hosseini, P. Dehghanian, Dynamic uncertainty set characterization for bulk power grid flexibility assessment, IEEE Syst. Journal 14 (1) (2020) 718–728.
[22] A. Abrantes, G. Gross, Towards the construction of a class of grid operational flexibility metrics, Elect. Power Syst. Res. 190 (2021) 106674.
[23] T. Heggarty, J.-Y. Bourmaud, R. Girard, G. Kariniotakis, Quantifying power system flexibility provision, Appl. Energy 279 (2020) 115852.
[24] H. Nosair, F. Bouffard, Energy-centric flexibility management in power systems, IEEE Trans. Power Syst. 31 (6) (2016) 5071–5081.
[25] B. P. Mukhoty, V. Maurya, S. K. Shukla, Sequence to sequence deep learning models for solar irradiation forecasting, 2019 IEEE Milan PowerTech (2019) 1–6.
[26] R. Yu, J. Gao, M. Yu, W. Lu, T. Xu, M. Zhao, et al., LSTM-EFG for wind power forecasting based on sequential correlation features, Future Gen. Computer Syst. 93 (2019) 33–42.
[27] Z. Qin, Y. Hou, S. Lei, F. Liu, Quantification of intra-hour security-constrained flexibility region, IEEE Trans. Sustain. Energy 8 (2) (2016) 671–684.
[28] S. Sreekumar, K. C. Sharma, R. Bhakar, Gumbel copula based multi interval ramp product for power system flexibility enhancement, Int. J. Elect. Power & Ene. Syst. 112 (2019) 417–427.
[29] S. Yamujala, A. Jain, R. Bhakar, J. Mathur, P. Kushwaha, Operational flexibility enhancement through flexible ramp products from energy storage, 2019 8th Int. Conf. on Power Syst. (2019) 1–5.
[30] A. Graves, Supervised sequence labelling with recurrent neural networks, 1^{st} ed. Springer (2012).
[31] J. Brownlee, Long Short-term Memory Networks with Python: Develop Sequence Prediction Models with Deep Learning, Machine Learning Mastery, 2017. Available: https://books.google.co.in/books?id=ONpdswEACAAJ.
[32] S. Patterson, S. Yeh, SAS ® Markov Chain Monte Carlo (MCMC) simulation in practice, Paper SP07 (2007).
[33] M. Ghamsary, K. Oda, L. Beeson, Fitting statistical models with PROC MCMC, SASGF (2020).
[34] Modern-era retrospective analysis for research and application,version 2 (MERRA V2), Accessed: 05-04-2019. [Online]. Available: `http://www.soda-pro.com/webservices`.
[35] CAISO (California) hourly actual and forecast demand, Accessed: 05-04-2019. [Online]. Available: `http://www.caiso.com/`.
[36] J. M. Morales, A. J. Conejo, H. Madsen, P. Pinson, M. Zugno, Integrating renewables in electricity markets: Operational problems, Vol. 205, Springer Science & Business Media, 2013.
[37] Pinnapuram integrated renewable energy with storage project, Tech. rep., Accessed: 20-06-2019. [Online]. Available: `http://environmentclearance.nic.in/` (2018).
[38] Y. Sumanth, A. Jain, P. Das, R. Bhakar, J. Mathur, P. Kushwaha, Operational strategy of energy storage to address day-ahead scheduling errors in high re scenario, in: 2018 8th IEEE India International Conference on Power Electronics (IICPE), IEEE, 2018, pp. 1–6.